

# A High Isolation Dual-Polarized Base Station Antenna with Wideband Differential Feed

Hua Chen\*, Quan Wang, Mankang Xue, Xinhui Yang, Ning Huang, and Qing Fang

*Faculty of Science, Kunming University of Science and Technology, Kun Ming, China*

**ABSTRACT:** In this paper, a novel stacked wideband differentially feed antenna with dual polarizations is designed for base station. The circular parasitic patch deepens the resonance depth by slotting. Two linear dipoles are placed at  $\pm 45^\circ$  under the circular parasitic patch to reduce the overall size of the antenna. The antenna introduces a cross-shaped differential feed to achieve high port isolation. Finally, the designed antenna is fabricated and tested. The test results show that the differential reflection coefficient  $|S_{dd11}|$  is more than 15 dB. The antenna achieves a differential impedance bandwidth of 53.1% (1.63 GHz–2.8 GHz). The isolation is greater than 42 dB over the entire operating bandwidth. The antenna also has a stable gain of  $8.2 \pm 0.4$  dBi and a half-power beamwidth of  $65^\circ \pm 4^\circ$ .

## 1. INTRODUCTION

Today, the communication environment is becoming more and more complex, and signal will inevitably produce attenuation or distortion in the transmission process, so in the base station, it is usually chosen to use a variety of polarized signal transmission to form an independent channel, to ensure the quality of communication. Dual-polarized antenna has the advantages of resisting multipath fading and increasing the capacity of a wireless communication system, so it is widely used in base station construction. In the construction of base stations, operators often require that the antenna be compact in size and low profile. In terms of performance, a wide operating bandwidth, high gain, high isolation, and stable radiation characteristics are required [1–6].

Considering the low-cost construction of base stations, microstrip patch antennas and vibrator antennas are widely used in base stations. The patch antennas proposed in [7–9] could achieve high isolation and wide impedance bandwidth, but they have the problem of high profile and narrow bandwidth. Even if using the multi-mode resonance technology to widen the bandwidth, introducing additional load will still result in parasitic radiation and distortion of the main radiation pattern. To solve the above problems, many dipole antennas have been reported in recent years. Ref. [10] proposes utilizing the strong mutual coupling between two dipoles to achieve impedance matching and sufficiently high isolation. Based on this method, a four-leaf clover dual-polarized antenna [11] and a dual-polarized antenna [12] feed by a Y-coupling are proposed. A  $\Gamma$ -coupled feed with a balun structure is reported to improve the stability of the antenna [13]. Because the feeding structure of the above antenna is asymmetric, the pattern will be deviated, and the isolation of the antenna is not ideal.

To avoid the above problems, some differentially fed antennas are proposed [14–24]. The antennas proposed in [14–16] adopt differential feed structures and could achieve a high gain, wide frequency band, and low profile. However, all the above antennas excited by differential feed are unipolar, which is not suitable for the current base station. Then, the broadband differentially fed antennas with dual polarizations are proposed in [17–24]. In [17], the planar antenna enhances the bandwidth by introducing four pairs of parasitic elements. The antenna has a high isolation of 45 dB, but the half-power beamwidth is  $65^\circ \pm 8^\circ$ , and the radiation pattern is relatively divergent. It is reported that the slot-stacked patch antenna applied to the base station has realized an impedance bandwidth of 49.4% (1.66–2.75 GHz) [18]. A broadband dual polarization slot antenna is designed based on the theory of aperture characteristic mode [19]. By introducing two pairs of differentially fed capacitive coupling elements to excite the two modes, the bandwidth is increased from 17% to 46%. In [20], an octagonal patch is designed as a radiation patch, and an H-slot and a differentially fed structure are used to adjust impedance matching. The designed antenna has a high isolation of more than 43 dB and an impedance bandwidth of 20.3% (3.14–3.81 GHz). A novel antenna in [21] adopts a cross-feeding structure and a parasitic element to achieve an impedance bandwidth of 52% (1.7–2.9 GHz) with a return loss of more than 14 dB, but its isolation is only 26 dB. A compact broadband differentially fed dual polarization antenna with high common mode suppression is reported in [22]. The impedance bandwidth of 55.3% (1.66–2.93 GHz) is achieved by using two orthogonal placed baluns connected with two open-end stubs as the feed network. In [23], two differential pairs of L-probes are inserted into a laminated resonator antenna (LRA) to excite degenerate dominant modes in LRA for dual-polarized operation. the designed antenna achieves a wide bandwidth of 29% with a differential reflection coefficient of less than  $-10$  dB. Ref. [24] pro-

\* Corresponding author: Hua Chen (cherrychen40600@163.com).

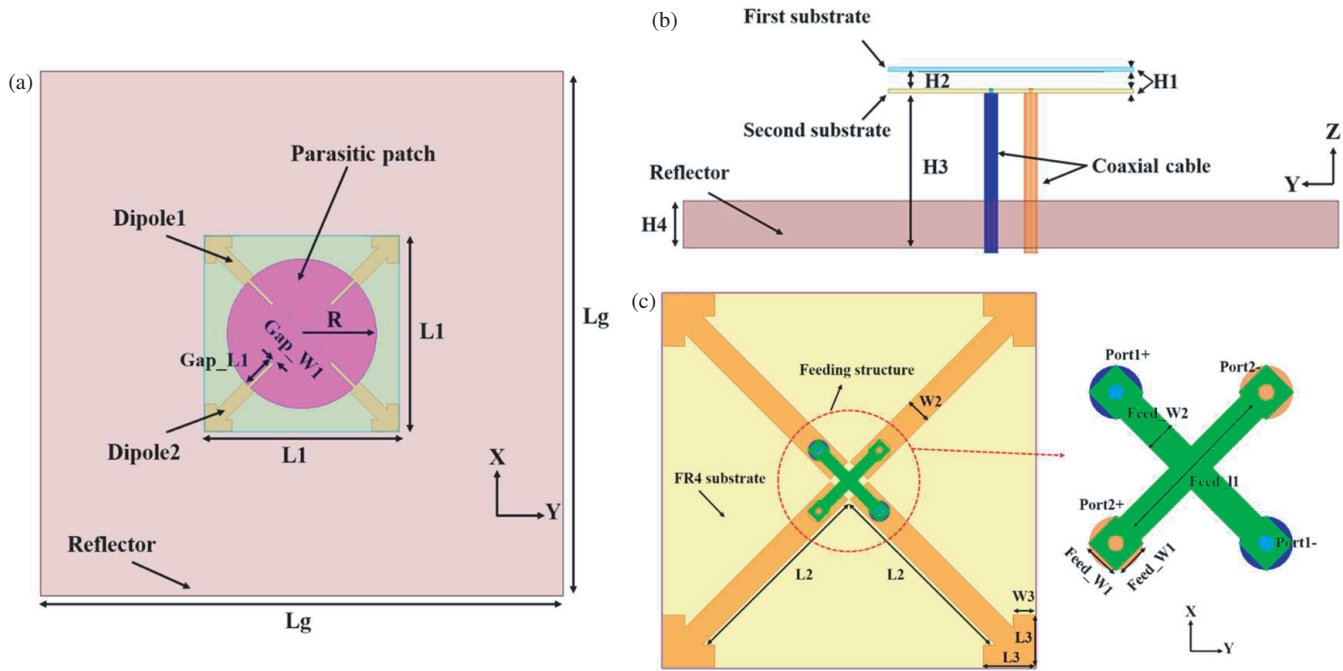


**FIGURE 1.** (a) Antenna top view. (b) Antenna side view. (c) Linear dipole and cross-shaped feeding structure.

poses a novel dual-polarized shared-aperture antenna array with a wide bandwidth (BW) by carefully designing and tightly arranging the elements with an overlapped BW of 25.4% from 23 to 29.7 GHz for the two orthogonal polarizations, a peak gain of 19.8 dBi, and an isolation larger than 18 dB. In [25], the structure consists of a simple patch and multiple split-ring resonant cavity metamaterials, with performance optimized by adjusting the height of the overlayer and the thickness of the metamaterial rings, achieving a minimum reflection coefficient of  $-49$  dB, a bandwidth of 490 MHz, and a maximum electric field intensity of  $1.29 \times 10^4$  V/m, demonstrating good directivity and a broad radiation pattern. In [26], a terahertz multiple-input multiple-output (MIMO) antenna is developed using metamaterials. The proposed two-port antenna incorporates complementary split-ring resonator patches, achieving a peak gain of 10.34 dB, along with broadband performance, high gain, and high isolation. In [27], a novel bent S-shaped metamaterial MIMO antenna design is proposed with an average effective gain of  $\leq -3.0$  dB, a total active reflection coefficient of  $\leq -10.0$  dB, a diversity gain of approximately 10 dB, a channel capacity loss of  $< 0.5$  bps/Hz/s, and an envelope correlation coefficient of  $< 0.01$ , exhibiting high gain and multi-band characteristics, making it suitable for high-speed wireless communication applications.

In this paper, a novel dual polarization microstrip antenna with differential feed is proposed. The polarization of the patch antenna is excited by a cross-type differential feed with equal amplitude and different phases. A circular parasitic patch with a slot enhances the impedance bandwidth of the antenna. The co-simulation results show that the impedance bandwidth is 53.1% (1.63–2.8 GHz), and the return loss is smaller than  $-15$  dB. The isolation between ports is greater than 46 dB. The antenna has

a stable radiation pattern and a 3 dB beamwidth of  $65^\circ \pm 4^\circ$ . The gain of the antenna is  $8.2 \pm 0.4$  dBi. The antenna structure designed in this paper is described in detail in Section 2.

## 2. ANTENNA STRUCTURE

Figure 1 shows the structure of the proposed antenna in this paper. A circular parasitic patch is printed on the bottom of the first dielectric plate. A cross-shaped feeding structure is printed on the upper surface of the second dielectric plate, and a linear dipole is printed on the lower surface. Port1+ and Port1– are a pair of differentially paired ports. Port2+ and Port2– are another. The inner conductor of the four ports coaxial cable is connected to the cross-shaped feeding structure, and the outer conductor is connected to the linear dipole. To reduce the size of the antenna, the linear dipoles are placed at  $\pm 45^\circ$ , respectively, and arrows are used at the ends of the linear dipoles to increase the electrical length of the current. In this paper, a novel dual polarization antenna is proposed on a metal reflector to achieve directional radiation.

A differentially fed dual-polarized antenna can be modeled as a single-ended four-port network, from which the  $S$ -parameters of the four ports can be extrapolated to determine the corresponding differential reflection coefficients,  $S_{dd11}$  and  $S_{dd22}$ .

$$S_{dd11} = (S(1+, 1+) - S(1+, 1-) - S(1-, 1+) + S(1-, 1-))/2 \quad (1)$$

$$S_{dd12} = (S(1+, 2+) - S(1+, 2-) - S(1-, 2+) + S(1-, 2-))/2 \quad (2)$$

$$S_{dd21} = (S(2+, 1+) - S(2+, 1-) - S(2-, 1+) + S(2-, 1-))/2$$

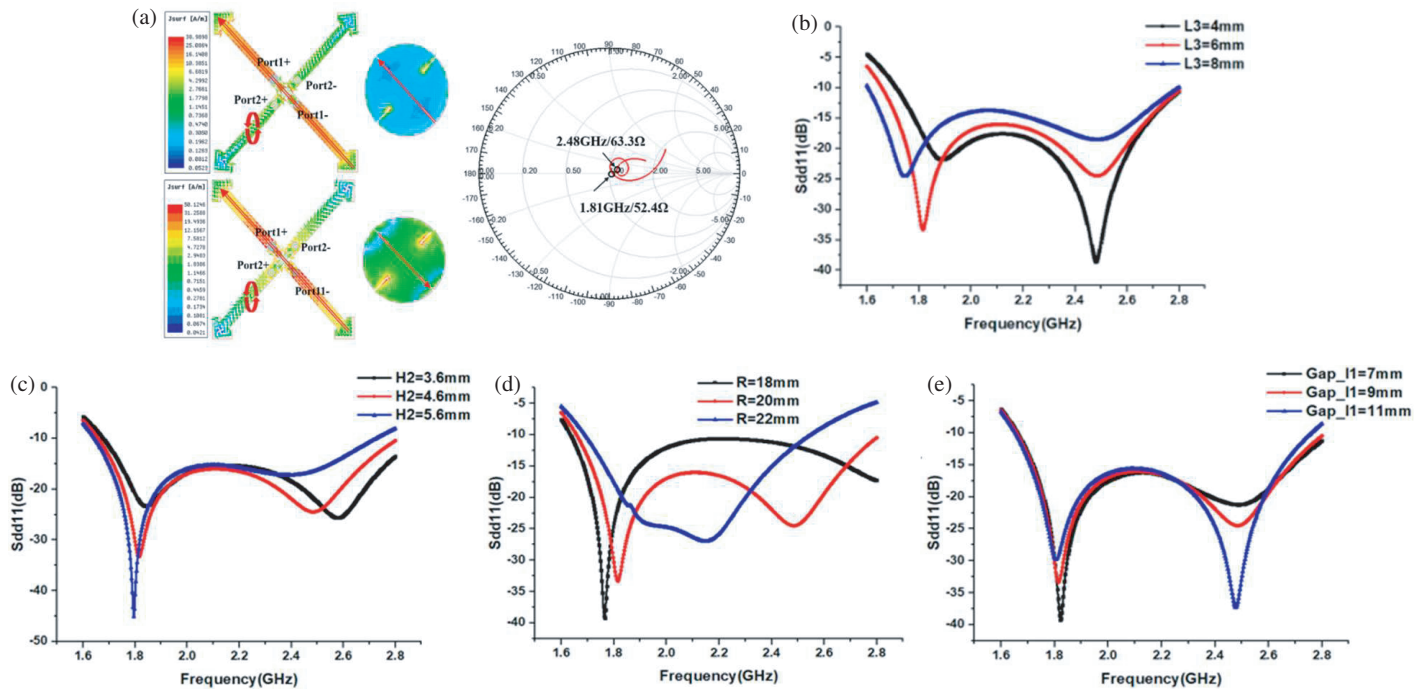


**FIGURE 2.** (a) 1.81 GHz and 2.48 GHz antenna current distribution and Smith chart. (b) Scanning analysis of the arrow length  $L_3$ . (c) Scanning analysis of the height  $H_2$ . (d) Scanning analysis of the radius  $R$ . (e) Scanning analysis of the slot line length  $\text{Gap}_{l1}$ .

Parameter	$L_1$	$L_2$	$L_3$	$\text{slot}_{w1}$	$\text{slot}_{l1}$	$H_2$	$H_3$
Value (mm)	52.3	33	6	1	9	4.6	33
Parameter	$H_4$	$W_2$	$W_3$	$\text{Feed}_{w1}$	$\text{Feed}_{w2}$	$\text{Feed}_{l1}$	$R$
Value (mm)	10	3.5	3	2.2	1.7	9.8	20
Parameter	$L_g$	$H_1$					
Value (mm)	140	1					

**TABLE 1.** Key parameters of the proposed antenna.

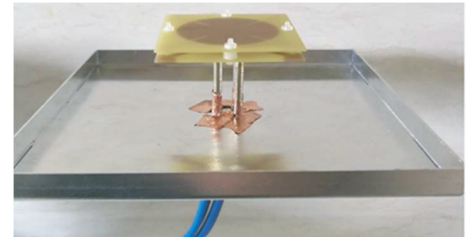


**FIGURE 3.** Physical antenna.

**TABLE 2.** Comparison of the proposed antenna and reference antennas ( $\lambda$  is the wavelength of the central frequency free space).

Ref.	Dimension ( $\lambda^3$ )	Bandwidth	Isolation (dB)	Gain (dBi)	HPBW (deg.)
[10]	$2.29 \times 1.11 \times 0.28$	57.5% (VSWR < 1.5)	> 31	$8.8 \pm 0.3$	NG
[11]	$1.47 \times 0.985 \times 0.265$	45% ( $ S_{11}  < -15$ dB)	> 30	$\sim 8.5$	$\sim 65^\circ$
[12]	$1.03 \times 1.03 \times 0.25$	45% (VSWR < 1.5)	> 25	$8.2 \pm 0.6$	$68^\circ \pm 2^\circ$
[13]	$1.1 \times 1.1 \times 0.238$	48% ( $ S_{11}  < -15$ dB)	> 22	$\sim 8.2$	$62.5^\circ \pm 3.5^\circ$
[21]	$1.03 \times 1.03 \times 0.25$	52% (VSWR < 1.5)	> 26.3	$\sim 8$	$65^\circ \pm 5^\circ$
Pro.	$1.03 \times 1.03 \times 0.24$	53.1% (VSWR < 1.5)	> 42	$8.2 \pm 0.4$	$65^\circ \pm 4^\circ$

$$-S(2-, 1+) + S(2-, 1-))/2 \quad (3)$$

$$S_{dd22} = (S(2+, 2+) - S(2+, 2-) - S(2-, 2+) + S(2-, 2-))/2 \quad (4)$$

To better understand the working principle of the antenna, the current distribution of the antenna is shown in Fig. 2(a) when it works at two resonance points. In addition, the key parameters of the antenna are scanned and optimized with the aid of

ANSYS HFSS Electromagnetics Suite 18.0, and the results are shown in Figs. 2(b)–(e). To meet the better performance of the designed antenna, we choose the arrow length  $L_3 = 6$  mm, the distance between the circular parasitic patch and the dipole  $H_2 = 4.6$  mm, the circular parasitic patch radius  $R = 20$  mm, and the slot line length  $\text{Gap}_{l1} = 9$  mm. The final design parameters are listed in Table 1. The next section shows the results of our antenna simulations and measurements.

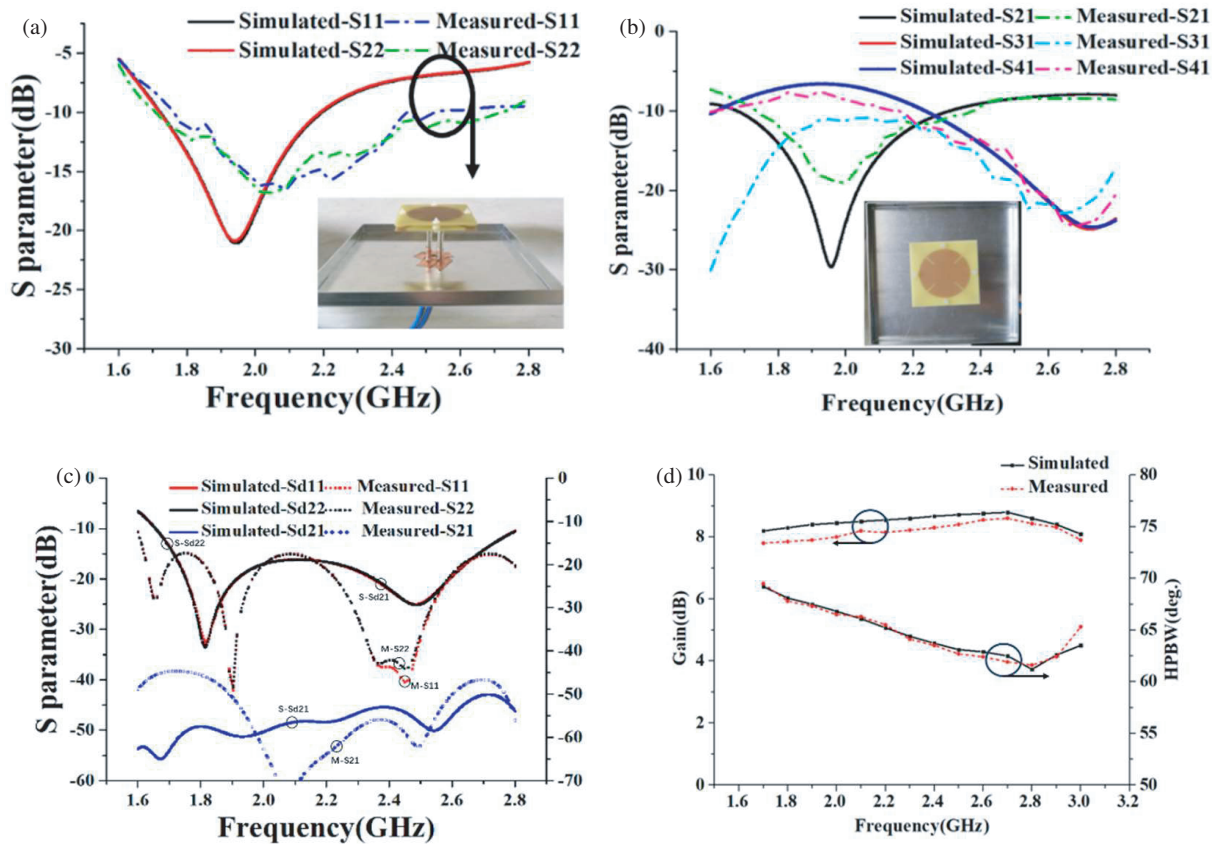


**FIGURE 4.** (a) Simulated and measured  $S$ -parameters of  $S_{11}$  and  $S_{22}$ . (b) Simulated and measured  $S$ -parameters of  $S_{21}$ ,  $S_{31}$  and  $S_{41}$ . (c) Simulated and measured the isolation and return loss of the four-port antenna. (d) Simulated and measured gains and HPBWs of the antenna.

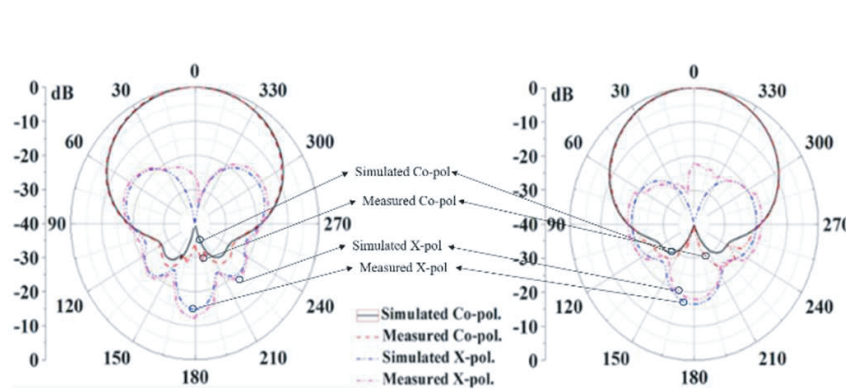


**FIGURE 5.** Radiation patterns of simulated antennas at 1.7 GHz and 2.7 GHz.

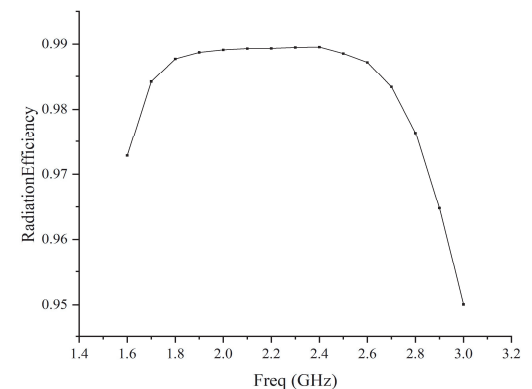


**FIGURE 6.** Radiation efficiency of the simulated antenna.

### 3. SIMULATION AND MEASUREMENT RESULTS

The antenna is fabricated and measured to verify the performance of the designed antenna. Fig. 3 shows the physical antenna. The curves in Figs. 4(a)–(b) show the simulated and measured four-port  $S$ -parameters. The antenna has a symmetrical structure, and we measured the  $S$ -parameters of  $S_{11}$ ,  $S_{22}$ ,  $S_{21}$ ,  $S_{31}$ ,  $S_{41}$ . It can be seen that the trends of the measurement and simulation results are basically the same, but there is a frequency offset. Firstly, it is because we measure the antenna in the laboratory, and the laboratory environment is not

ideal. There are some environmental factors. Secondly, there is a processing error in the process of antenna manufacturing, and the coaxial cable was lengthened. Finally, there is an error in the measurement, which is difficult to avoid. The return loss of the antenna in the 1.63–2.8 GHz band is above 14 dB in Fig. 4(c). The antenna port isolation is greater than 42 dB. Fig. 4(d) depicts the simulated and measured gain curves and 3 dB beamwidths of the antenna. The measured gain is above 7.8 dBi, which is smaller than the simulated gain. The difference could come from the power distribution network. The



3 dB beamwidth measured at  $+45^\circ$  is maintained at  $65^\circ \pm 4^\circ$ , and a stable beamwidth is obtained in the entire operating band.

The radiation pattern of the final antenna test is shown in Fig. 5. The radiation patterns of the  $H$ -plane at 1.7 GHz and 2.7 GHz are shown in Fig. 4. Due to the symmetry of the ports and structure, we have only drawn the  $+45^\circ$  polarization pattern. From the Figure can see that the antenna has a stable radiation pattern. The axial cross-polarization ratio is less than  $-30$  dB, and the cross-polarization ratio of  $\pm 60^\circ$  is less than  $-9$  dB.

A comparison of the recommended antenna with the reference antenna is shown in Table 2. Compared with the reference antenna, the antenna designed in this paper achieves higher isolation; the circular parasitic patch deepens the resonance depth by slotting; and the antenna structure is more compact. The antenna gain in [10] is higher. However, the isolation degree of [10] is lower than the antenna proposed in this paper. The antenna designed in this paper is also smaller in size than that in [10]. The above comparison shows that the antenna designed in this paper has the advantages of small size, high isolation, and stable beamwidth.

The radiation efficiency of the simulated antenna is shown in Fig. 6, demonstrating the antenna's stability and high radiation efficiency.

#### 4. CONCLUSION

In this paper, a wideband differentially fed parasitic patch antenna is proposed. The antenna size is  $52.3 \times 52.3 \times 33$  mm. Measurement and simulation results both show that the impedance bandwidth of the antenna is 53.1% (VSWR  $< 1.5$ ) in the range of 1.63–2.8 GHz. The isolation between ports is greater than 42 dB. It has a stable gain ( $8.2 \pm 0.4$  dBi) and stable half-power beamwidth ( $65^\circ \pm 4^\circ$ ). The miniaturization of antennas is one of the main directions of today's research, and this paper reduces the size of the antenna but provides better isolation and ensures a stable gain compared to previous antennas of larger size, which is certainly valuable. Also, the antenna is less costly due to PCB fabrication. This will be a good choice for future base station systems using differential signalling.

#### ACKNOWLEDGEMENT

This project was supported by the Yunnan Provincial Foundation Program (202201AT070202) and the Yunnan Fundamental Research Projects (202201AU070144 and 202301BE070001-005).

#### REFERENCES

- [1] Luo, Y., Q.-X. Chu, and D.-L. Wen, "A plus/minus 45 degree dual-polarized base-station antenna with enhanced cross-polarization discrimination via addition of four parasitic elements placed in a square contour," *IEEE Transactions on Antennas and Propagation*, Vol. 64, No. 4, 1514–1519, Apr. 2016.
- [2] Luo, Y. and Q.-X. Chu, "Oriental crown-shaped differentially fed dual-polarized multidipole antenna," *IEEE Transactions on Antennas and Propagation*, Vol. 63, No. 11, 4678–4685, Nov. 2015.
- [3] Ding, C., H. Sun, R. W. Ziolkowski, and Y. J. Guo, "Simplified tightly-coupled cross-dipole arrangement for base station applications," *IEEE Access*, Vol. 5, 27 491–27 503, 2017.
- [4] Zhang, H., D. Ding, and X. Y. Zhang, "Broadband dual-polarized antenna with stable radiation patterns for base station applications," *IEEE Antennas and Wireless Propagation Letters*, Vol. 22, No. 2, 337–341, Feb. 2023.
- [5] Wu, S. and F. Shang, "Broadband dual-polarized magnetoelectric dipole antenna with compact structure for 5G base station," *IEEE Access*, Vol. 11, 20 806–20 813, 2023.
- [6] Chen, Z., T. Xu, J.-F. Li, L. H. Ye, and D.-L. Wu, "Dual-broadband dual-polarized base station antenna array with stable radiation pattern," *IEEE Antennas and Wireless Propagation Letters*, Vol. 22, No. 2, 303–307, Feb. 2023.
- [7] Li, J., S. Yang, Y. Gou, J. Hu, and Z. Nie, "Wideband dual-polarized magnetically coupled patch antenna array with high port isolation," *IEEE Transactions on Antennas and Propagation*, Vol. 64, No. 1, 117–125, Jan. 2016.
- [8] Deng, J.-Y., L.-X. Guo, Y.-Z. Yin, J. Qiu, and Z.-S. Wu, "Broadband patch antennas fed by novel tuned loop," *IEEE Transactions on Antennas and Propagation*, Vol. 61, No. 4, 2290–2293, Apr. 2013.
- [9] Xie, J.-J., Y.-Z. Yin, J.-H. Wang, and X.-L. Liu, "Wideband dual-polarised electromagnetic-fed patch antenna with high isolation and low cross-polarisation," *Electronics Letters*, Vol. 49, No. 3, 171–173, Jan. 2013.
- [10] Bao, Z., Z. Nie, and X. Zong, "A novel broadband dual-polarization antenna utilizing strong mutual coupling," *IEEE Transactions on Antennas and Propagation*, Vol. 62, No. 1, 450–454, Jan. 2014.
- [11] Cui, Y., R. Li, and H. Fu, "A broadband dual-polarized planar antenna for 2G/3G/LTE base stations," *IEEE Transactions on Antennas and Propagation*, Vol. 62, No. 9, 4836–4840, Sep. 2014.
- [12] Chu, Q.-X., D.-L. Wen, and Y. Luo, "A broadband  $\pm 45^\circ$  dual-polarized antenna with y-shaped feeding lines," *IEEE Transactions on Antennas and Propagation*, Vol. 63, No. 2, 483–490, 2015.
- [13] Huang, H., Y. Liu, and S. Gong, "A broadband dual-polarized base station antenna with sturdy construction," *IEEE Antennas and Wireless Propagation Letters*, Vol. 16, 665–668, 2016.
- [14] Li, M. and K.-M. Luk, "A differential-fed UWB antenna element with unidirectional radiation," *IEEE Transactions on Antennas and Propagation*, Vol. 64, No. 8, 3651–3656, Aug. 2016.
- [15] White, C. R. and G. M. Rebeiz, "A differential dual-polarized cavity-backed microstrip patch antenna with independent frequency tuning," *IEEE Transactions on Antennas and Propagation*, Vol. 58, No. 11, 3490–3498, Nov. 2010.
- [16] Liao, S., P. Wu, K. M. Shum, and Q. Xue, "Differentially fed planar aperture antenna with high gain and wide bandwidth for millimeter-wave application," *IEEE Transactions on Antennas and Propagation*, Vol. 63, No. 3, 966–977, Mar. 2015.
- [17] Cui, Y., X. Gao, and R. Li, "A broadband differentially fed dual-polarized planar antenna," *IEEE Transactions on Antennas and Propagation*, Vol. 65, No. 6, 3231–3234, Jun. 2017.
- [18] Tang, Z., J. Liu, Y.-M. Cai, J. Wang, and Y. Yin, "A wideband differentially fed dual-polarized stacked patch antenna with tuned slot excitations," *IEEE Transactions on Antennas and Propagation*, Vol. 66, No. 4, 2055–2060, Apr. 2018.
- [19] Wang, C., Y. Chen, and S. Yang, "Bandwidth enhancement of a dual-polarized slot antenna using characteristic modes," *IEEE Antennas and Wireless Propagation Letters*, Vol. 17, No. 6, 988–992, Jun. 2018.

- [20] Liu, Y., S. Wang, X. Wang, and Y. Jia, "A differentially fed dual-polarized slot antenna with high isolation and low profile for base station application," *IEEE Antennas and Wireless Propagation Letters*, Vol. 18, No. 2, 303–307, Feb. 2019.
- [21] Wen, D.-L., D.-Z. Zheng, and Q.-X. Chu, "A wideband differentially fed dual-polarized antenna with stable radiation pattern for base stations," *IEEE Transactions on Antennas and Propagation*, Vol. 65, No. 5, 2248–2255, May 2017.
- [22] Zhou, Z., Z. Wei, Z. Tang, Y. Yin, and J. Ren, "Compact and wideband differentially fed dual-polarized antenna with high common-mode suppression," *IEEE Access*, Vol. 7, 108 818–108 826, 2019.
- [23] Hou, Y., Z. Shao, Y. Zhang, and J. Mao, "A wideband differentially fed dual-polarized laminated resonator antenna," *IEEE Transactions on Antennas and Propagation*, Vol. 69, No. 7, 4148–4153, Jul. 2021.
- [24] Wang, M. and C. H. Chan, "A novel differentially-fed dual-polarized shared aperture antenna array," *IEEE Transactions on Antennas and Propagation*, Vol. 70, No. 12, 12 276–12 281, Dec. 2022.
- [25] Armghan, A., S. Lavadiya, M. Alsharari, K. Aliqab, M. G. Daher, and S. K. Patel, "Highly efficient and multiband metamaterial microstrip-based radiating structure design showing high gain performance for wireless communication devices," *Crystals*, Vol. 13, No. 4, 674, 2023.
- [26] Armghan, A., K. Aliqab, M. Alsharari, O. Alsalman, J. Parmar, and S. K. Patel, "Design and development of ultrabroadband, high-gain, and high-isolation THz MIMO antenna with a complementary split-ring resonator metamaterial," *Micromachines*, Vol. 14, No. 7, 1328, 2023.
- [27] Armghan, A., M. Alsharari, K. Aliqab, A. H. M. Almawgani, M. Irfan, and S. K. Patel, "Multiband and high gain meandered metamaterial THz MIMO antenna for highspeed wireless communication applications," *Optical and Quantum Electronics*, Vol. 55, No. 9, 828, 2023.